Multisensor data fusion for impact-echo testing of concrete structures

2012 Smart Mater. Struct. 21 075021

(http://iopscience.iop.org/0964-1726/21/7/075021)

IOP PUBLISHING SMART MATERIALS AND STRUCTURES
Smart Mater. Struct. **21** (2012) 075021 (7pp) doi:10.1088/0964-1726/21/7/075021

Multisensor data fusion for impact-echo testing of concrete structures

Ying Zhang[1], Xiangmin Wei[1], Yi-Te Tsai[2], Jinying Zhu[2], Farhad A Fetrat[3] and Nenad Gucunski[3]

[1] School of Electrical and Computer Engineering, Georgia Institute of Technology, GA 31407, USA
[2] Department of Civil, Architectural and Environmental Engineering, University of Texas at Austin, Austin, TX 78712, USA
[3] Department of Civil and Environmental Engineering, Rutgers University, New Brunswick, NJ 08901, USA

E-mail: yzhang@gatech.edu

Received 6 December 2011, in final form 25 May 2012
Published 14 June 2012
Online at stacks.iop.org/SMS/21/075021

Abstract
Based on the investigation of spatial variations of impact-echo signals for different source and receiver locations, a simple multisensor data fusion strategy is proposed to increase the accuracy of nondestructive evaluation of concrete structures using the impact-echo test. The data fusion strategy fuses the ratios between spectral amplitudes of the delamination and concrete bottom echo signals (D/B ratios) from multiple source–receiver arrays. The fused D/B ratios demonstrate different characteristics for test locations above the delamination, above the sound concrete, and across the delamination boundary. These characteristics can be used to accurately locate the delamination and its boundaries without increasing testing time. The applicability of the multisensor data fusion for impact-echo testing is validated using both numerical simulation and experimental testings.

(Some figures may appear in colour only in the online journal)

1. Introduction

According to the Federal Highway Administration, 146 633 out of 604 474 bridges in the United States are deficient as of December 2010 [1]. Enormous financial and human resources are required for their maintenance. One of the most common problems in concrete bridge decks is corrosion-induced deck delamination [2]. Impact-echo (IE) has been widely accepted as an effective nondestructive evaluation (NDE) method for delamination detection. Compared with other traditional NDE methods for delamination detection, such as chain dragging or hammer sounding, the IE method is advantageous because it can provide quantitative information about the delamination depth and detect early signs of delamination.

In the IE test, a transducer is used to measure the surface response of a concrete slab when a mechanical impact is applied on the surface nearby. The IE mode is usually interpreted as multiple reflections of the compression (P) wave between the top and bottom surfaces of the plate. If a delamination exists beneath the test point, the IE mode will be built between the delamination and the top surface. The time domain signal measured by the transducer is transformed to the frequency domain using Fourier transformation, and the peak frequency is obtained from the Fourier spectrum. The IE peak frequency (f) can be used to estimate the depth of the reflector (D), which corresponds to either the bottom surface of a concrete slab or internal defects,

$$D = \frac{\beta V_P}{2f} \qquad (1)$$

where V_P is the P-wave velocity in the concrete and β is an empirical correction factor, which is approximately 0.96 for plate-like structures [3]. The correction factor was described as a result of an excitation of a particular mode (the thickness mode) of vibration in the plate by Lin and Sansalone [4]. However, Gibson and Popovics [5] later found the IE resonant frequency corresponds to the zero group velocity frequency of the first symmetrical Lamb mode (S1) in a plate structure. They also successfully explained the β factor using the Lamb wave theory, and found that the β factor depends on Poisson's ratio of the material in plate structures.

The IE method is commonly used for NDE of concrete structures by conducting point testing on a grid of selected spacing [6]. The evaluation of the condition at each test point is based on the IE test results for that particular point. If the dominant peak in the frequency spectrum of the signal corresponds to the IE frequency f_B from the bottom of the concrete structure, the concrete at the test point is generally considered as sound, i.e. there is no internal defect. If the frequency of the dominant peak in the frequency spectrum is higher than the bottom echo frequency, it indicates a high probability of having an internal defect under the test point. If the test point is above a delamination with a high size to depth ratio, the frequency of flexural mode oscillations will dominate the frequency spectrum of the corresponding signal. Since the frequency of the dominating flexural mode is usually lower than the bottom echo frequency, and has very high amplitudes in most cases, this phenomenon can be applied to identify a relatively large shallow delamination without defect depth information. However, the defect depth can be calculated by identifying the delamination echo frequency f_D after removing the low frequency flexural mode. This general approach can provide relatively accurate results, if both the impact source and receiver are on a sound section of a deck, or above the defect region not near the delamination boundary. If the test point is close to the delamination boundary, the interpretation of the IE signal is challenging due to wave scattering and mode conversions at the delamination boundary, which may lead to erroneous interpretation of the IE test results [7].

Data fusion techniques have been applied to various NDE applications to reduce the signal uncertainty and increase evaluation accuracy [8]. The basic approaches for data fusion include the fusion of data from different types of NDE sensors [9] and the fusion of data from the same type of sensors under different conditions [10]. For the NDE of concrete structures, data fusion has been used to combine various NDE technologies [11, 12] or integrate ground penetrating radar (GPR) data with different testing conditions [13]. However, to the best knowledge of the authors of this paper, few have investigated the use of data fusion to improve the accuracy of the IE test. Although some research has been performed to use visualization for advanced data presentation [14–16], the main idea was to integrate the frequency spectra (or the corresponding depth spectra) of the individual test data into one platform for the overall condition assessment. The simple visualization platform alone cannot increase detection accuracy around the delamination boundary.

In this paper, the spatial variations of IE signals are first investigated for various source and receiver locations using numerical simulation data. Based on the investigation, a multisensor data fusion strategy is proposed to improve the accuracy of the IE test results using multiple source–receiver arrays, especially to determine the delamination boundary. The feasibility of the fusion strategy is further validated by IE experimental results.

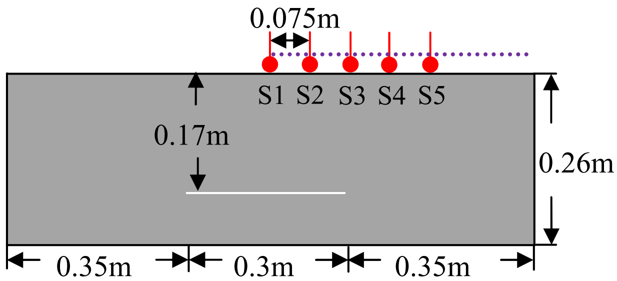

Figure 1. Numerical simulation model to investigate effects of source and receiver locations in the IE test.

2. Numerical simulation of the IE test

2.1. Numerical simulation model

To develop multisensor data fusion strategies for delamination detection, numerical simulations were performed to simulate a concrete slab with a delamination. The spatial variations of surface responses were investigated when an impact was applied at different locations. The cross-section of the numerical simulation model is shown in figure 1. The concrete slab was modeled using 3D solid elements, and analyzed using the finite element analysis software ABAQUS. The model has lateral dimensions of 1 m $\times$ 1 m and a thickness of 0.26 m. The absorbing boundary conditions were imposed at the four edges of the concrete slab to avoid wave reflection from these boundaries. Therefore, the simulated concrete slab can be considered as being infinitely long and wide. The delamination was 0.3 m $\times$ 0.3 m, 0.17 m deep, and located at the center of the concrete slab. The Young's modulus, mass density and Poisson's ratio of the concrete were 50 GPa, 2500 kg m^{-3}, and 0.2, respectively. The P-wave velocity was 4714 m s^{-1}. According to equation (1), the corresponding IE frequencies for the delamination and the slab bottom are 13.3 kHz and 8.7 kHz, respectively. In the finite element analysis, an impact force was applied at one of the five source locations indicated by S1, S2, S3, S4 and S5. S1 is at the center of the concrete slab surface. The distance between two adjacent source locations was 0.075 m. For each impact source location, the surface response (out-of-plane velocity) was evaluated every 0.01 m along the centerline, starting from the center of the slab towards the edge of the slab. The test line is indicated by the dotted line in figure 1. The time increment used in the analysis was 1 μs.

2.2. Simulation results

As the surface response signal contains a strong surface wave component, which may affect the echo signal interpretation, the surface waves are first reduced in all IE signals by applying a Hanning window to the time domain signals. The starting point of the Hanning window is calculated from the surface wave velocity and the distance between the test point and the impact location. After the surface wave components are reduced, all signals are transformed into the frequency domain. The echo frequencies from the delamination and the

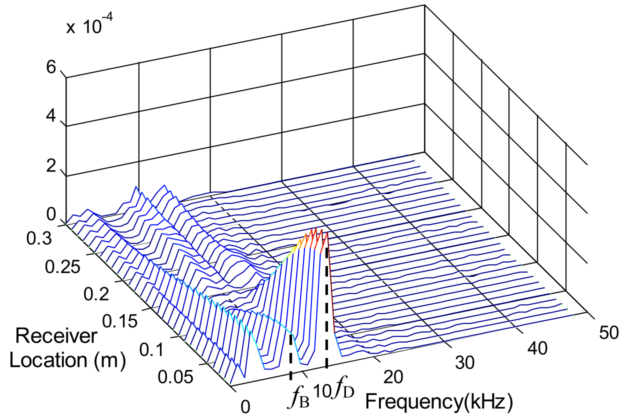

Figure 2. Frequency spectra of the response at different receiver locations to an impact applied at S1.

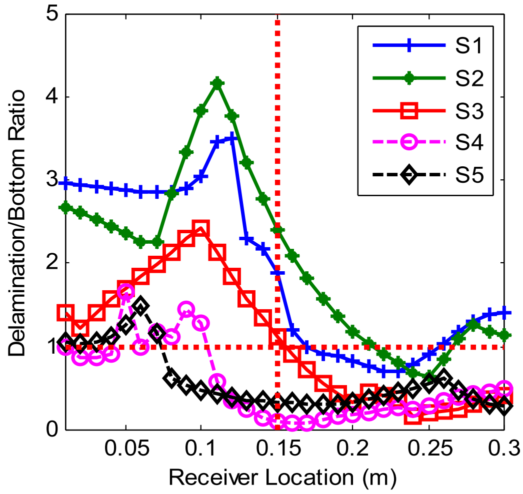

Figure 3. The spatial variation of the D/B ratio from IE numerical simulation.

bottom of the concrete slab can be clearly identified using the frequency spectra of the receiver array. As an example, frequency spectra of the response between 0.01 m and 0.30 m away from the surface center of the slab to an impact applied at S1 are shown in figure 2. Two dominant peaks marked as f_B and f_D agree with the calculated IE frequencies 8.7 kHz and 13.3 kHz corresponding to the bottom of the deck and the delamination depth.

Based on analysis and observations of spatial variations of IE signals for different source locations, the ratio between spectral amplitudes at the delamination echo frequency f_D and the bottom echo frequency f_B (D/B ratio) was considered as a feasible feature parameter for multisensor data fusion. The bottom echo signal here also serves as a normalization factor to alleviate the non-consistency effect caused by amplitude differences of the mechanical impact that may vary from one test point to another. As frequency shift may happen in the IE test, if there was no frequency peak corresponding to the delamination or bottom echo frequency exactly, the adjacent frequency peaks might be considered based on the test location and the evaluation of the frequency spectra of the adjacent test points. For a signal in which the bottom echo signal was too small to be discernible, the value near the expected deck bottom echo frequency in the frequency spectrum was used as the bottom echo signal. Since this may only happen when the test point is above the delamination, this operation does not affect the data fusion results, as shown in section 3. A similar strategy was applied to the delamination echo signal, if the frequency peak is too small when the receiver is far away from the delamination area.

The spatial distributions of the D/B ratio for different source locations are shown in figure 3. The origin is the center of the concrete slab, the point above the delamination center. The delamination boundary is 0.15 m away from the origin. The region between 0.15 m and 0.30 m is the sound deck section. Figure 3 shows that the D/B ratio is greater than 1 when both source (S1 and S2) and receiver locations are on the delaminated deck section, and less than 1 when both source (S4 and S5) and receiver locations are on the sound section. When the D/B ratio has a value greater than 1, it indicates the delamination echo signal is the dominant peak frequency in the spectrum. If the D/B ratio is less than 1, the bottom echo signal dominates the spectrum. As mentioned earlier, if the deck bottom echo signal dominates, it is generally considered that there is no internal defect under the test point. When both source and receiver locations are above the defect region or the sound deck, the simulation results support the general defect identification rules used in the current IE testing. However, when the source location is above the delamination and the receiver is on the sound deck section, the D/B ratio is greater than 1 near the delamination boundary and oscillates around 1 when the receiver moves away from the delamination. When the source location is on the sound deck section and the receiver is above the delaminated region, the D/B ratio is less than 1 near the delamination boundary and could have a value above 1 for receivers far into the region above the delaminated area. For the conventional IE interpretation of individual test point results, it may provide misleading results when the test point is near the delamination boundary.

The spatial variation of the surface response for a single impact source also shows that the D/B ratio decreases continuously across a wide region when the receiving position is around the delamination boundary while moving away from the delamination center. This could be used as a feature to roughly identify the delamination boundary using a single source with a receiver array. However, the delamination boundary location cannot be accurately determined by this approach. Besides, it is usually not encouraged to set receivers too far away from the impact source in the IE test.

3. Multisensor data fusion

As shown in figure 3, when both the source and receiver are above the delamination or the sound deck section, there is no difficulty of interpreting the test results. But when the source and receiver locations are on the opposite sides of the delamination boundary, the testing result may be misleading. Additionally, when the receiver is close to the delamination boundary, no matter whether it is inside or

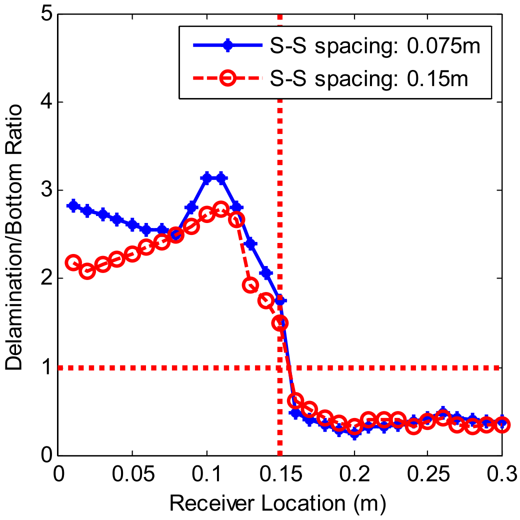

Figure 4. Multisensor data fusion results for IE numerical simulation (S–S spacing indicates the distance between two adjacent sources).

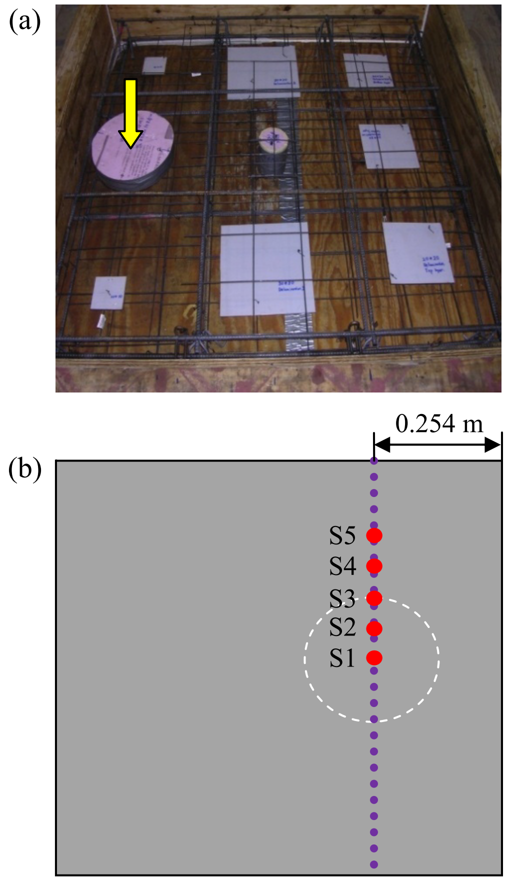

Figure 5. IE experimental setup: (a) internal defects before casting concrete; and (b) targeted delamination and impact source locations.

outside the delamination boundary, the D/B ratio is larger than 1 with an impact applied inside the delamination boundary, and less than 1 with an impact applied outside the delamination boundary. It demonstrates a complementary effect for the boundary region when the source is located inside or outside the delamination boundary. Based on this observation, a simple multisensor data fusion strategy is proposed to effectively combine the information from multiple source–receiver arrays to increase the accuracy of the defect detection. In this proposed fusion method, the D/B ratio of a test point is calculated by averaging the D/B ratios of two signals obtained at the same test point but generated by two adjacent impacts one at a time. These two impact source locations are on the opposite sides of the test point (receiver position). For example, the D/B ratio for a test point between S1 and S2 (0–0.075 m) is the average value of two corresponding D/B ratios obtained at the same test point caused by S1 and S2; and the D/B ratio for a point in the region between S2 and S3 is the average value of two corresponding D/B ratios caused by S2 and S3. If both sources and receivers are above the delamination or above the sound concrete, D/B ratios of all receivers will be larger or less than 1, respectively. Taking the average does not change whether the D/B ratio is greater or less than 1. However, the results in the transition region across the delamination boundary will be improved due to the complementary effect caused by two impacts applied inside and outside the delamination area.

The solid line in figure 4 shows the fused D/B ratios from all five source–receiver arrays, fused in the following four regions: S1–S2, S2–S3, S3–S4 and S4–S5. The fused D/B ratio is largely greater than 1 when the receiver is above the delamination, and has a sharp decrease across the delamination boundary. The fused D/B ratio is quickly reduced to a value less than 1 once the receiver crosses the delamination boundary, and stabilizes afterwards with only minor oscillations. The multisensor data fusion results provide an accurate determination of the delamination boundary without any ambiguity, and the precision of the delamination boundary is determined by the receiver spatial resolution. To evaluate whether increasing the distance between two adjacent sources affects the result, sources S2 and S4 are removed from the fusion process. The distance between adjacent source locations (S1, S3 and S5) is increased to 0.15 m. The fused D/B ratios from these three source–receiver arrays are plotted using the dashed line in figure 4. Although the absolute value of the fused D/B ratio for a particular location changes slightly compared to the fused results from the five source–receiver arrays, it does not change the trend of the spatial variation of the fused D/B ratio. The delamination region and boundary can still be accurately identified.

4. Experimental validation

4.1. Experimental setup

To validate the multisensor data fusion strategy developed from the numerical simulation, laboratory experiments were performed on a concrete slab with embedded artificial defects. The internal defects before casting the concrete are shown in figure 5(a). To be comparable to the simulation setup, the circular delamination (indicated by the yellow arrow) was selected as the target since it had sufficient distance from two adjacent small defects to perform the source–receiver array experiment similar to the simulation. The concrete slab was flipped over after casting as the bottom provides a smooth testing surface. Figure 5(b) shows the plan view of the concrete slab and the targeted internal defect location from the testing surface. The concrete slab was 1.524 m × 1.524 m and had a thickness of 0.26 m. The circular delamination had a diameter of 0.3 m and was 0.17 m deep. The P-wave velocity was measured as 4459 m s^{-1}. The corresponding echo frequencies from the delamination and the bottom of the slab were 12.6 kHz and 8.2 kHz respectively, which were close to the numerical simulation values.

As in the simulations, the impact was applied at five locations, as shown in figure 5(b). A wire-mounted solid steel ball of 11 mm in diameter was used as the impact source, which is effective in generating stress waves in concrete in the frequency range of interest (up to 20 kHz). The first source location (S1) was above the center of the delamination. The distance between two adjacent sources was 0.075 m. For each impact source location, the response was measured at 18 locations with nine test points on each side of the source along the dotted test line, as shown in figure 5(b). The distance between two adjacent receivers on each side was 0.025 m. The sampling frequency was 1 MHz. The response at most test locations was measured using an air-coupled sensor (PCB model 377B01 microphone) [17] except the test locations that were 0.025 and 0.05 m away from the impact source due to the size of the air-coupled sensor. The response at these four locations for each source was measured using a contact accelerometer (PCB 352C65). As the accelerometer measured the particle acceleration, the D/B ratio calculated from the acceleration signal was converted to the D/B ratio of the corresponding velocity. Each IE test was repeated multiple times to guarantee the repeatability of the testing results. The signals were acquired using an NI-USB 5133 oscilloscope.

4.2. Experimental results and discussions

The spatial distributions of the D/B ratio for different source locations are shown in figure 6. The origin is the test point above the delamination center. The responses are plotted along the test line starting from the origin. For each source location, the surface response at the source location was estimated using linear interpolation. Although there are small deviations between the experimental and simulation results due to the noisy experimental environment, inhomogeneous materials and other unexpected factors, the general trend is similar to that of the numerical simulation. When both the source and receiver are above the delamination or the sound slab section far away from the delamination boundary, the single source–receiver pair provides reasonable defect detection results. In the region around the delamination boundary, it is difficult to make a correct assessment from the single source–receiver pair. Combining the results from five source–receiver arrays, it is possible for a user to identify the delamination boundary from figure 6. However, it is difficult to establish a criterion to automatically determine

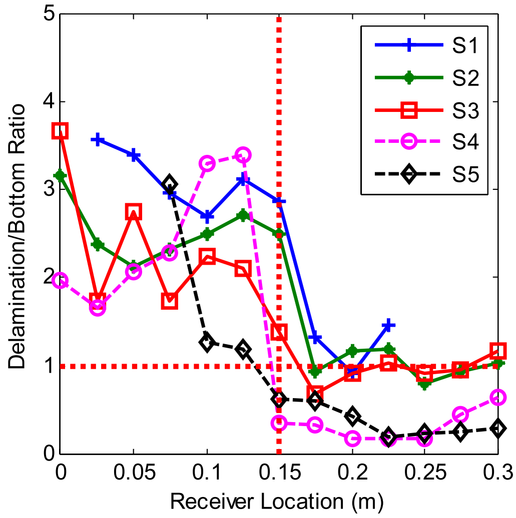

Figure 6. The spatial variations of the D/B ratio from IE experimental testing.

the delamination boundary, which is important for testing large concrete structures. Additionally, it is impractical and uneconomical to attach a long receiver array to each impact source.

The multisensor data fusion strategy developed in section 3 was applied to the experimental data. The solid line in figure 7(a) shows the fused results from five source–receiver arrays, with an adjacent source distance of 0.075 m. The simulation results are plotted as a dashed line for comparison. The distance between two adjacent receivers is 0.025 m in the experiment, while the simulation results are plotted every 0.03 m for comparison. Figure 7(a) shows that the spatial variation of the fused D/B ratio has a similar trend for both the simulation and experiment. The fused D/B ratio is greater than 1 for test points above the delamination, and drops to a value less than 1 when the test point is outside the delamination area. The fused D/B ratio has a sharp change when the test point moves across the delamination boundary, and stabilizes afterwards. This provides a precise determination of the delamination boundary. Figure 7(b) shows the fused results as the distance between adjacent sources increases to 0.15 m. The experimental result also matches that of the simulation. The same rules can be used to accurately determine the delamination boundary. Figure 7 also demonstrates that the criteria used for delamination boundary determination will not be affected by reducing the number of receivers.

5. Conclusions

The spatial variations of the IE signals are investigated for different source and receiver locations. Based on the investigation, the ratio between the echo signals from the delamination and the bottom of the concrete slab (D/B ratio) is selected as a feature parameter to support multisensor data fusion for IE testing. A simple multisensor data fusion strategy is proposed to fuse the D/B ratios of IE signals

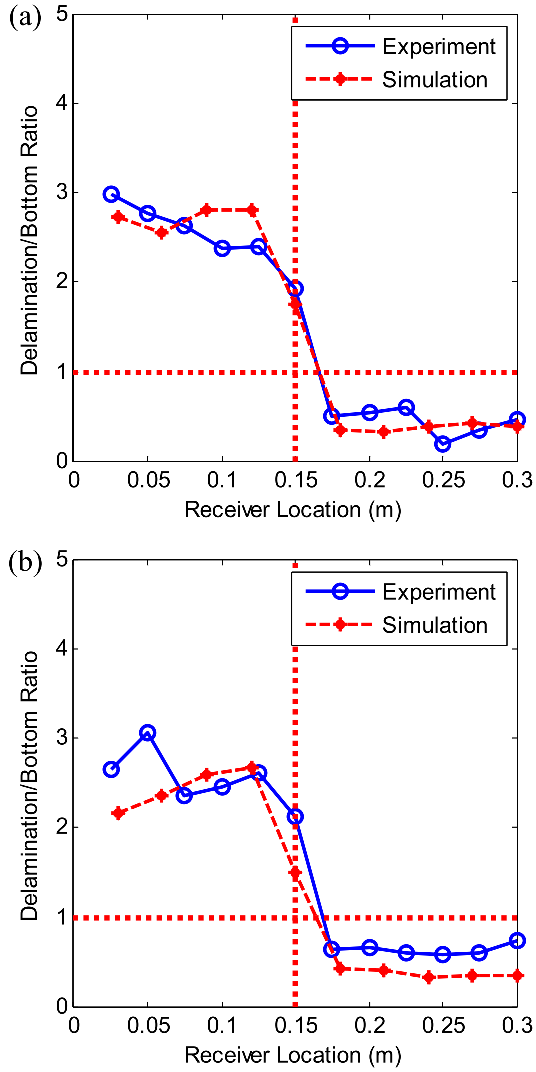

Figure 7. Comparison of multisensor data fusion results between simulation and experiment: (a) adjacent source distance is 0.075 m; and (b) adjacent source distance is 0.150 m.

from multiple source–receiver arrays. Both the simulation and experimental results demonstrate that the fused D/B ratio shows a sharp decrease around the boundary, which can be used to determine delamination boundaries and automate the delamination detection process for large concrete structures. The boundary resolution is determined by the receiver spatial resolution in the source–receiver arrays.

It should be noted that the D/B ratio also depends on the frequency spectrum of the input force. If the frequency spectrum of the input force varies significantly at different test locations, further normalization needs to be adopted to compensate relative differences between the input energies at frequencies corresponding to the bottom and delamination echo frequencies. If the frequency spectrum of the input force is similar at different test locations, which was the case in this study, further normalization is not necessary. The reason is that it only changes the absolute value of the D/B ratio and does not affect its trend. The delamination boundary is determined based on the change of the D/B ratio.

This study has also shown that increasing the distance between adjacent sources within a reasonable range does not decrease the accuracy of the multisensor data fusion result. This is the case if the receiver resolution does not change and all receivers are within an acceptable distance from the corresponding impact source. This indicates that the IE resolution can be increased with the multiple source–receiver array approach without increasing the testing time. As the receiver array simultaneously measures the response at different locations, the testing time is controlled by the number of source locations.

IE testing using source–receiver arrays also provides a way to remove abnormal signals from the test results. In practice, IE signals may be complicated by noise and the inhomogeneity characteristics of the material. The spatial variation of IE signals shows that the IE signal should have a relatively smooth change if receivers are close to each other. This feature can be used to remove abnormal signals by comparing adjacent receiver signals.

Acknowledgments

This research was supported in part by the US Department of Commerce, National Institute of Standards and Technology (NIST), Technology Innovation Program (TIP).

References

[1] FHWA, National Bridge Inventory, US Department of Transportation, December 2010 www.fhwa.dot.gov/bridge/nbi/defbr10.cfm#c
[2] Gucunski N, Slabaugh G, Wang Z, Fang T and Maher A 2008 Impact echo data from bridge deck testing: visualization and interpretation *Transp. Res. Rec.* **2050** 111–21
[3] Sansalone M J and Streett W B 1997 *Impact-Echo—Nondestructive Evaluation of Concrete and Masonry* (New York: Bullbrier Press)
[4] Lin J M and Sansalone M J 1996 Impact-echo studies of interfacial bond quality in concrete: part 1—effects of unbonded fraction *ACI Mater. J.* **93** 223–32
[5] Gibson A and Popovics J S 2005 Lamb wave basis for impact-echo method analysis *J. Eng. Mech.* **131** 438–43
[6] Gucunski N, Slabaugh G, Wang Z, Fang T and Maher A 2008 Visualization and interpretation of impact echo data from bridge deck testing *Transp. Res. Rec.* **2050** 11–121
[7] Shokouhi P 2006 Comprehensive evaluation of concrete bridge decks using impact echo *PhD Dissertation* Rutgers University
[8] Liu Z, Forsyth D S, Komorowski J P, Hanasaki K and Kirubarajan T 2007 Survey: state of the art in NDE data fusion techniques *IEEE Trans. Instrum. Meas.* **56** 2435–51
[9] Song Y W and Udpa S S 1996 A new morphological algorithm for fusing ultrasonic and eddy current images *Proc. 1996 IEEE Ultrason. Symp. (San Antonio, TX, Nov.)* pp 649–52
[10] Mina M, Yim J, Udpa S S, Udpa L, Lord W and Sun K 1996 Two dimensional multi-frequency eddy current data fusion *Review of Progress in QNDE* vol 15 (New York: Plenum) pp 2125–32
[11] Kohl C, Krause M, Maierhofer C and Wöstmann J 2005 2D- and 3D-visualisation of NDT-data using data fusion technique *Mater. Struct.* **38** 817–26
[12] Kohl C and Streicher D 2006 Results of reconstructed and fused NDT-data measured in the laboratory and on-site at bridges *Cem. Concr. Compos.* **28** 402–13

[13] Hugenschmidt J and Kalogeropoulos A 2009 The inspection of retaining walls using GPR *J. Appl. Geophys.* **67** 335–44

[14] Zhu J and Popovics J S 2007 Imaging concrete structures using air-coupled impact-echo *J. Eng. Mech.* **133** 628–40

[15] Liu P L and Yeh P L 2011 Spectral tomography of concrete structures based on impact echo depth spectra *NDTE Int.* **44** 692–702

[16] Gucunski N, Yan M, Wang Z, Fang T and Maher A 2012 Rapid bridge deck condition assessment using three-dimensional visualization of impact echo data *J. Infrastruct. Syst.* **18** 12–24

[17] Kee S H and Zhu J 2010 Using air-coupled sensors to determine the depth of a surface-breaking crack in concrete *J. Acoust. Soc. Am.* **127** 1279–87